[4] C. Desai and S. S. Williamson, "Optimal design of a parallel hybrid electric vehicle using multi-objective genetic algorithms," in *Proc. IEEE VPPC*, 2009, pp. 871–876.
[5] E. Vinot *et al.*, "Improvement of an EVT-based HEV using dynamic programming," *IEEE Trans. Veh. Technol.*, vol. 63, no. 1, pp. 40–50, Jan. 2014.
[6] R. Bellman, *Dynamic Programming*. Princeton, NJ, USA: Princeton Univ. Press, 1957.
[7] D. Bertsekas, *Dynamic Programming and Optimal Control*. Belmont, MA, USA: Athena Scientific, 1995.
[8] D. E. Kirk, *Optimal Control Theory*. New York, NY, USA: Dover, 2012.
[9] J. Scordia *et al.*, "Global optimisation of energy management laws in hybrid vehicles using dynamic programming," *Int. J. Veh. Design*, vol. 39, no. 4, pp. 349–367, 2005.
[10] M. Koot *et al.*, "Energy management strategies for VEHICULAR electric power systems," *IEEE Trans. Veh. Technol.*, vol. 54, no. 13, pp. 771–782, May 2005.
[11] L. V. Perez, G. R. Bossio, D. Moitre, and G. O. Garcia, "Optimization of power management in an hybrid electric vehicle using dynamic programming," *Math. Comput. Simul.*, vol. 73, no. 1–4, pp. 244–254, Nov. 2006.
[12] J. M. Miller, "Hybrid electric vehicle propulsion system architectures of the e-CVT type," *IEEE Trans. Power Electron.*, vol. 21, no. 3, pp. 756–767, May 2006.
[13] B. Mashadi and S. A. Emadi, "Dual-mode power-split transmission for hybrid electric vehicles," *IEEE Trans. Veh. Technol.*, vol. 59, no. 7, pp. 3223–3232, Sep. 2010.
[14] M. J. Hoeijmakers and J. A. Ferreira, "The electric variable transmission," *IEEE Trans. Ind. Appl.*, vol. 42, no. 4, pp. 1092–1100, Jul./Aug. 2006.
[15] Y. Cheng, C. Espanet, R. Trigui, A. Bouscayrol, and S. Cui, "Design of a permanent magnet electric variable transmission for HEV applications," in *Proc. IEEE VPPC*, 2010, pp. 1–5.
[16] Y. Cheng, R. Trigui, C. Espanet, A. Bouscayrol, and S. Cui, "Specifications and design of a PM electric variable transmission for Toyota Prius II," *IEEE Trans. Veh. Technol.*, vol. 60, no. 9, pp. 4106–4114, Nov. 2011.
[17] A. Ghayebloo and A. Radan, "Superiority of dual mechanical ports machine based structure for series-parallel hybrid electric vehicle applications," *IEEE Trans. Veh. Technol.*, to be published.
[18] C. Shu-Mei, H. Wen-Xiang, and Z. Qian-Fan, "Research on power density improvement design of an HEV using induction machine based electrical variable transmission," in *Proc. IEEE VPPC*, 2008, pp. 1–4.
[19] G. Xizheng, W. Xuhui, Z. Feng, and F. Tao, "Comparison of two different structure of permanent magnet dual mechanical port machine," in *Proc. IEEE VPPC*, 2008, pp. 1–5.
[20] K. Muta, M. Yamazaki, and J. Tokieda, "Development of new-generation hybrid system THS II-drastic improvement of power performance and fuel economy," Soc. Automotive Eng. Int., Warrendale, PA, USA, Tech. Rep., 2004.
[21] E. Vinot, J. Scordia, R. Trigui, B. Jeanneret, and F. Badin, "Model simulation, validation and case study of the 2004 THS of Toyota Prius," *Int. J. Veh. Syst. Model. Test.*, vol. 3, no. 3, pp. 139–167, 2008.
[22] B. Jeanneret, R. Trigui, F. Badin, and F. Harel, "New hybrid concept simulation tools, evaluation on the Toyota Prius car," in *Proc. 16th Int. Electr. Veh. Symp.*, Beijing, China, 1999, pp. 1–11.
[23] S. Kermani, R. Trigui, S. Delprat, B. Jeanneret, and T. M Guerera, "PHIL implementation of energy management optimization for a parallel HEV on a predefined route," *IEEE Trans. Veh. Technol.*, vol. 60, no. 3, pp. 782–792, Mar. 2011.

Spectrum Sensing of OFDM Signals in the Presence of Carrier Frequency Offset

Weiyang Xu, Wei Xiang, *Senior Member, IEEE*, Maged Elkashlan, *Member, IEEE*, and Hani Mehrpouyan, *Member, IEEE*

***Abstract*—This paper addresses the important issue of detecting orthogonal frequency-division multiplexing (OFDM) signals in the presence of carrier frequency offset (CFO). The proposed algorithm utilizes the characteristics of the covariance matrix of the discrete Fourier transform of the input signal to the detector to determine the presence of the primary user's signal. This algorithm can be exploited to differentiate OFDM signals from the noise through the proposal of a new decision metric, which measures the off-diagonal elements of the input signal's covariance matrix. The decision threshold subject to a given probability of false alarm is derived, whereas performance analysis is carried out to demonstrate the potential of the proposed algorithm. Finally, simulation results are presented to validate the effectiveness of the proposed sensing method in comparison with other existing approaches.**

***Index Terms*—Carrier frequency offset (CFO), cognitive radio (CR), covariance matrix, orthogonal frequency-division multiplexing (OFDM), spectrum sensing.**

I. INTRODUCTION

Sensing the presence of the primary user's signal is one of the most critical and challenging tasks in cognitive radio (CR). Existing algorithms can be generally classified into methods of matched-filter detection, energy detection, and feature detection [1]. Recently, a new detection method has been proposed, which uses eigenvalues of the signal covariance matrix [2]. This approach is shown to perform well when the signals to be detected are mutually correlated [3].

Orthogonal frequency-division multiplexing (OFDM) has been considered as a promising candidate for implementing the physical layer of CR due to its capability of transmitting over noncontiguous frequency bands. However, sensing OFDM signals proves to be more challenging due to its multicarrier characteristics. Currently, existing schemes make use of either the cyclic prefix (CP) [4], [5] or pilot tones in OFDM symbols [6], [7]. In [4], Lei *et al.* introduced a decision metric with the aid of the CP and derived the generalized likelihood ratio test (GLRT) for this decision metric. Bokharaiee *et al.* proposed a constrained GLRT by using the multipath correlation among the primary signals [5]. Unfortunately, the performance of

Manuscript received March 18, 2015; revised May 28, 2015; accepted September 8, 2015. Date of publication September 14, 2015; date of current version August 11, 2016. This work was supported by the National Natural Science Foundation of China under Grant 61201177. The review of this paper was coordinated by Dr. C. Ibars.

W. Xu is with the College of Communication Engineering, Chongqing University, Chongqing 400044, China (e-mail: weiyangxu@cqu.edu.cn).

W. Xiang is with the School of Mechanical and Electrical Engineering, University of Southern Queensland, Toowoomba, Qld. 4350, Australia (e-mail: wei.xiang@usq.edu.au).

M. Elkashlan is with the School of Electronic Engineering and Computer Science, Queen Mary University of London, London E1 4NS, U.K. (e-mail: maged.elkashlan@qmul.ac.uk).

H. Mehrpouyan is with the Department of Electrical and Computer Engineering, Boise State University, Boise, ID 83725 USA (e-mail: hani.mehr@ieee.org).

Digital Object Identifier 10.1109/TVT.2015.2478517

the CP-based schemes will degrade substantially if the length of the CP is reduced to enhance spectral efficiency. Relying on pilot tones, a detection scheme that utilizes the cross correlation among the time-domain symbols was suggested in [6]. Moreover, a pilot-aided second-order cyclostationary detection algorithm was derived in [7], demonstrating a superior performance. However, since pilots are usually pseudorandomly coded and uniquely dedicated to the primary transmission, it is nontrivial or even impossible for cognitive users to obtain this information accurately. More importantly, all the aforementioned methods fail to take into account the carrier frequency offset (CFO). In general, solutions to tackle the CFO can be divided into two categories. The first category estimates and compensates for the CFO errors before spectrum sensing. For example, Chen *et al.* employed the CP-based synchronization method to compensate for the CFO [8]. However, the estimation accuracy severely degrades because the detector often works in highly noisy environments. The second category exploits hybrid domain signal processing algorithms to design spectrum sensing schemes robust to the CFO, but pilot symbols are required to be perfectly known to the cognitive users [9].

In this paper, we focus on the detection of OFDM signals in CR systems in consideration of the CFO. The major contributions of this paper are summarized as follows.

1) A new decision metric robust to the CFO is introduced, which is based on the covariance matrix of the discrete Fourier transform (DFT) of the detector's input vector;
2) A decision threshold is computed according to the required probability of false alarm. A performance analysis concerning the detection probability and computational complexity of the proposed method is also carried out.

The remainder of this paper is organized as follows. Section II describes the OFDM-based CR system model. A new decision metric is proposed based on the covariance matrix in Section III. The detection probability and complexity of the proposed detector are analyzed in Section IV. Sections V and VI present the numerical results and conclude this paper, respectively.

Notation: Lower- and uppercase symbols are used for time- and frequency-domain signals, respectively. $(\cdot)^*$, $(\cdot)^T$, and $(\cdot)^H$ denote conjugate, transpose, and conjugate transpose, respectively. $\mathbf{F}_N$, $\mathbf{1}_N$, and $\mathbf{I}_N$ indicate the DFT matrix, the matrix of ones, and the identity matrix, respectively, all of size $N \times N$. $Q(x) = (2/\sqrt{\pi}) \int_x^\infty e^{-t^2} dt$ is the complementary error function. Finally, $\mathrm{E}[\cdot]$, $\| \cdot \|_{L_1}$ and $\odot$ are the expectation, L_1-norm and Hadamard product operators, respectively.

II. System Model and Problem Formulation

At the transmitter side, the samples of the ith OFDM symbol is given by

$$x_{i,n} = \frac{1}{\sqrt{N}} \sum_{k=0}^{N-1} X_{i,k} e^{j \frac{2\pi}{N} nk}, \qquad -N_g \leq n \leq N-1 \tag{1}$$

where $X_{i,k}$, which is assumed to have unit variance, represents the symbol modulating the kth subcarrier, and N_g is the length of the CP. The resultant baseband signal is upconverted to passband and propagates through the wireless environment. There usually exists the CFO in the received signal because of the mismatch between the transmitter and receiver's local oscillators or the Doppler effect. Therefore, the baseband discrete-time signal can be written as

$$r_{i,n} = e^{j \frac{2\pi}{N} n\varepsilon} \sum_{l=0}^{L-1} h_l x_{i,n-l} + w_{i,n} \tag{2}$$

where ε is the normalized CFO, h_l indicates the impulse response of the lth channel tap, L is the number of taps, and $w_{i,n}$ is the Gaussian noise with zero mean and variance σ_n^2. On the other hand, when no primary users are present, the received signal is simply equal to $w_{i,n}$.

Thus, sensing OFDM signals can be formulated as a binary hypothesis testing problem, i.e.,

$$\begin{aligned} \mathcal{H}_0 &: r_{i,n} = w_{i,n} \\ \mathcal{H}_1 &: r_{i,n} = d_{i,n} + w_{i,n} \end{aligned} \tag{3}$$

where $d_{i,n}$ is the received primary user's signal, and $\mathcal{H}_0$ and $\mathcal{H}_1$ indicate the absence and presence of the primary user, respectively. Since cognitive users may not have access to training symbols or pilots, it is unrealistic to assume perfect synchronization. As a result, the proposed sensing method should be designed to be resilient to the CFO.

III. Covariance-Matrix-Based Spectrum Sensing Algorithm

A. Properties of the Signal Covariance Matrix

The different properties of the signal covariance matrix in the frequency domain under $\mathcal{H}_0$ and $\mathcal{H}_1$ constitute the basis of our method. Let $\mathbf{w}_i \triangleq [w_{i,0}, \ldots, w_{i,N-1}]^T$ be the input vector under $\mathcal{H}_0$, it is readily shown that the covariance matrix of $\mathbf{W}_i = \mathbf{F}_N \mathbf{w}_i$ is $\sigma_n^2 \mathbf{I}_N$.

In the presence of primary user's signal, let $\mathbf{r}_i \triangleq [r_{i,0}, \ldots, r_{i,N-1}]^T$ be the N-point input vector of the detector after discarding the CP, then the DFT of $\mathbf{r}_i$ is given by

$$\mathbf{Y}_i = \mathbf{F}_N \mathbf{r}_i = \mathbf{F}_N \mathbf{\Phi}(\varepsilon) \mathbf{F}_N^H \mathbf{H} \mathbf{X}_i + \mathbf{W}_i \tag{4}$$

where

$$\begin{aligned} \mathbf{Y}_i &\triangleq [Y_{i,0}, \ldots, Y_{i,N-1}]^T \\ \mathbf{X}_i &\triangleq [X_{i,0}, \ldots, X_{i,N-1}]^T \\ \mathbf{H} &\triangleq \mathrm{diag}\{H_{i,0}, \ldots, H_{i,N-1}\} \\ \Phi(\varepsilon) &\triangleq \mathrm{diag}\left\{1, e^{j2\pi\varepsilon/N}, \ldots, e^{j2\pi(N-1)\varepsilon/N}\right\}. \end{aligned}$$

Here, $H_{i,k} = (1/\sqrt{N}) \sum_{l=0}^{L-1} h_l e^{-j2\pi kl/N}$, for $0 \leq k \leq N-1$, denotes the frequency response of the kth subcarrier. The channel is assumed to be constant during spectrum sensing. Therefore, the covariance matrix of $\mathbf{Y}_i$ can be represented by

$$\mathbf{R} = \mathbf{F}_N^H \mathbf{\Phi}(\varepsilon) \mathbf{F}_N \mathbf{H} \mathbf{H}^H \mathbf{F}_N^H \mathbf{\Phi}^*(\varepsilon) \mathbf{F}_N + \sigma_n^2 \mathbf{I}_N. \tag{5}$$

For better understanding, the kth element of $\mathbf{Y}_i$ is

$$Y_{i,k} = \sum_{t=0}^{N-1} I_{t-k}^{\varepsilon} X_{i,t} H_{i,t} + W_{i,k} \tag{6}$$

where

$$I_n^{\varepsilon} = \frac{\sin(\pi\varepsilon)}{N \sin\left(\frac{\pi}{N}(\varepsilon + n)\right)} \exp\left(j \frac{\pi}{N} \left((N-1)\varepsilon - n\right)\right).$$

Therefore, the (p,q)th entry of the covariance matrix can be written as

$$\mathbf{R}(p,q) = \begin{cases} \sum_{t=0}^{N-1} \left| I_{t-p}^{\varepsilon} H_{i,t} \right|^2 + \sigma_n^2, & p = q \\ \sum_{t=0}^{N-1} I_{t-p}^{\varepsilon} I_{t-q}^{\varepsilon *} |H_{i,t}|^2, & p \neq q. \end{cases} \tag{7}$$

It is evident that $\mathbf{R}$ is nondiagonal due to the intercarrier interference among subcarriers. However, when ε denotes the integer CFO, it can be derived that $\sum_{t=0}^{N-1} I_{t-p}^{\varepsilon} I_{t-q}^{\varepsilon *} |H_{i,t}|^2 = 0$. Hence, the covariance matrix is still diagonal under $\mathcal{H}_1$.

B. Proposed Spectrum Sensing Algorithm

Based on the aforementioned discussions, it can be concluded that if the detector's input contains the primary user's signal contaminated by the CFO, the covariance matrix is not diagonal, except when ε is an integer, as opposed to hypothesis $\mathcal{H}_0$, where only the noise is present. Hence, this property can be exploited to detect the primary user's signal by comparing the off-diagonal power of the covariance matrix with a preset threshold. Since $\mathbf{R}$ cannot be practically obtained, we resort to the sample covariance matrix $\hat{\mathbf{R}}$, which is computed by

$$\hat{\mathbf{R}} = \frac{1}{M}\sum_{i=1}^{M}\mathbf{Y}_i\mathbf{Y}_i^H \tag{8}$$

where M indicates the number of OFDM symbols. Thus, the decision metric can be written as

$$\zeta = \frac{\left\|\hat{\mathbf{R}}\odot(\mathbf{1}_N - \mathbf{I}_N)\right\|_{L_1}}{\sqrt{N^2-N}} \tag{9}$$

which is essentially the sum of magnitudes of (N^2-N) nondiagonal elements of $\hat{\mathbf{R}}$, and the denominator is the normalizing factor. Since γ is selected with respect to P_{fa}, the probability distribution function (pdf) under $\mathcal{H}_0$ needs to be fully established.

Lemma 1: It can be shown that if M is sufficiently large, the decision metric ζ in (9) can be approximated as a sum of $(N^2-N)/2$ *independent and identically distributed* (i.i.d.) Rayleigh variables under $\mathcal{H}_0$. (Please refer to Appendix A for detailed derivation.)

Based on Lemma 1, there is no closed-form expression for the pdf of ζ. Hence, we resort to a simple approximation outlined in [10]. Let $K=(N^2-N)/2$, the pdf of ζ can be approximated using the central limit theorem (CLT; for detailed derivation, please refer to Appendix A), i.e.,

$$p(\zeta|\mathcal{H}_0) \approx \frac{1}{\sqrt{2\pi}}e^{-\frac{1}{2}\left(\frac{\zeta-\mu_{\mathcal{H}_0}\sqrt{K}}{\sigma_{\mathcal{H}_0}}\right)^2} \tag{10}$$

where

$$\mu_{\mathcal{H}_0} = \sqrt{\frac{\pi}{4M}}\sigma_n^2 \quad \sigma_{\mathcal{H}_0}^2 = \left(1-\frac{\pi}{4}\right)\frac{\sigma_n^4}{M}.$$

Given a preset P_{fa}, the threshold γ is constrained by [11]

$$P_{\mathrm{fa}} = \int_{\gamma}^{\infty} p(\zeta|\mathcal{H}_0)d\zeta. \tag{11}$$

By substituting (10) into (11), we can calculate the decision threshold using

$$\gamma = Q^{-1}\left(\frac{2P_{\mathrm{fa}}}{\sigma_{\mathcal{H}_0}}\right)\sigma_{\mathcal{H}_0} + \mu_{\mathcal{H}_0}\sqrt{K}. \tag{12}$$

Equation (12) shows that γ relates to M, N, P_{fa}, and noise variance σ_n^2. Since we can choose the values of M, N, and P_{fa} before sensing, the only unknown is σ_n^2. To tackle this issue, a real-time noise power estimation scheme is exploited [12]. In OFDM, there are a few null subcarriers used as the guard band. Thus, the received signal power on such a null subcarrier is close to the noise power if there is no interference or out-of-band signal intrusion on the subcarrier. As the index of null subcarriers is available to cognitive users, we can choose these subcarriers for noise power estimation. With the estimate $\hat{\sigma}_n^2$, γ can be obtained before making a decision.

C. Spectrum Sensing With CFO Being an Integer Multiple of Subcarrier Spacing

For the complete study, the applicability of the our spectrum sensing algorithm in the presence of an integer CFO will be analyzed here.

Lemma 2: The proposed scheme works when the CFO is an integer multiple of subcarrier spacing. In this scenario, it is shown that the pdf of the decision metric can be represented as (for detailed derivation, please refer to Appendix A)

$$p_{\mathrm{IFO}}(\zeta|\mathcal{H}_1) \approx \frac{1}{\sqrt{2\pi}}e^{-\frac{1}{2}\left(\frac{\zeta-\mu_{\mathcal{H}_1}\sqrt{K}}{\sigma_{\mathcal{H}_1}}\right)^2} \tag{13}$$

where

$$\mu_{\mathrm{IFO},\mathcal{H}_1} = \sqrt{\frac{\pi}{4M}\left(\sigma_n^4 + 2\sigma_n^2\sigma_H^2\right)}$$
$$\sigma_{\mathrm{IFO},\mathcal{H}_1}^2 = \left(1-\frac{\pi}{4}\right)\frac{\left(\sigma_n^4 + 2\sigma_n^2\sigma_H^2\right)}{M}$$

with subscript "IFO" denoting the scenario with an integer CFO, and σ_H^2 being the variance of the channel frequency response. The proposed algorithm is expected to differentiate the primary user's signal from noise because $\mu_{\mathrm{IFO},\mathcal{H}_1} > \mu_{\mathcal{H}_0}$. Thus, (13) indicates that our scheme can detect the primary user's signal even in the presence of CFO that is an integer multiple of the subcarrier spacing. Note that the CFO-free scenario is a special case of Lemma 2 when $\varepsilon = 0$. In fact, although the proposed algorithm is designed to tackle the spectrum sensing with the CFO, its applicability in the absence of this error is also shown.

D. Timing Issue

The impact of timing offsets on our scheme needs to be addressed. Since $w_{i,n}$ is immune to timing offsets, the covariance matrix is still diagonal under $\mathcal{H}_0$. Under $\mathcal{H}_1$, the DFT window contains data from two consecutive OFDM symbols when the timing offset is outside the ISI-free region [13]. As a result, the independence among subcarriers is destroyed such that the covariance matrix becomes nondiagonal. According to our former analysis, the proposed algorithm works in this situation. The covariance matrix is diagonal if the timing offset resides in the ISI-free region. It can be shown that the proposed method in this scenario is applicable in a way similar to that in Section III-C. Therefore, it is concluded that the proposed scheme still works in the presence of timing offsets, which further enhances the practicality of the algorithm.

IV. Performance Analysis and Discussion

A. Probability of Detection and Complexity Analysis

The pdf of the decision metric under $\mathcal{H}_1$ is unavailable since it depends on the unknown CFO. However, without any loss of generality, we can assume that the frequency offset is evenly distributed in a certain range and can be integrated out to conduct performance analysis concerning P_d. Here, we assume that the CFO is evenly distributed over $(-0, 5, 0.5]$ [9].

It is proved that ζ in this scenario can be approximated as the sum of Ricean variables. The corresponding pdf is represented as (please refer to Appendix B for detailed derivation)

$$p(\zeta|\mathcal{H}_1) \approx \frac{1}{\sqrt{2\pi}}e^{-\frac{1}{2}\left(\frac{\zeta-\mu_{\mathcal{H}_1}\sqrt{K}}{\sigma_{\mathcal{H}_1}}\right)^2} \tag{14}$$

TABLE I
COMPARISON OF COMPLEX MULTIPLICATIONS AMONG SENSING ALGORITHMS

Algorithms	Number of complex multiplications
Proposed scheme	$MN\log_2 N/2 + MN^2$
Method in [4]	$M\,(N+N_g)^2$
Method in [6]	M^2N/z
Method in [8]	$MN_g\,(N+N_g) + MN\log_2\,(N) + M^2N/2z^2$

where

$$\mu_{\mathcal{H}_1} = L_{\frac{1}{2}}(-\nu^2)\sqrt{\frac{\pi}{4M}}\sigma_n^2$$
$$\sigma_{\mathcal{H}_1}^2 = \frac{\sigma_n^4}{M} + \frac{\sigma_n^4\nu^2}{M} - \frac{\pi\sigma_n^4}{4M}L_{\frac{1}{2}}^2(-\nu^2)$$
$$\nu = \frac{4\pi^2\sigma_n^2 N\sqrt{M}\sigma_H^2}{(\Gamma+\psi(N))^2 + \psi(1,N) - \pi^2/6}.$$

Here, $L_{1/2}(x) = e^{x/2}[(1-x)J_0(-x/2) - xJ_1(-x/2)]$ represents the Laguerre polynomial, with $J_p(\cdot)$ being the pth-order modified Bessel function of the first kind, Γ is the Euler–Mascheroni constant, and $\psi(\cdot)$ and $\psi(1,\cdot)$ denote the logarithmic derivatives of the gamma and trigamma functions, respectively. The fact that $\mu_{\mathcal{H}_1}$ is always larger than $\mu_{\mathcal{H}_0}$ in (10), which follows from $L_{1/2}(-\nu^2) > 1$, i.e., the argument of monotonically decreasing function $L_{1/2}(\cdot)$ is negative and $L_{1/2}(0) = 1$, lays the foundation for the proposed spectrum sensing scheme.

Given the pdf under $\mathcal{H}_1$, the probability of detection P_d is calculated by $\Pr\{\zeta > \gamma; \mathcal{H}_1\}$, i.e.,

$$P_d = \frac{1}{2}Q\left(\frac{\gamma - \mu_{\mathcal{H}_1}\sqrt{K}}{\sqrt{2}\sigma_{\mathcal{H}_1}}\right). \tag{15}$$

Moreover, P_d can be rewritten by substituting (12) into (15), i.e.,

$$P_d = \frac{1}{2}Q\left(\frac{Q^{-1}\left(2P_{\text{fa}}/\sigma_{\mathcal{H}_0}\right)\sigma_{\mathcal{H}_0} - (\mu_{\mathcal{H}_1} - \mu_{\mathcal{H}_0})\sqrt{K}}{\sqrt{2}\sigma_{\mathcal{H}_1}}\right). \tag{16}$$

It can be shown that P_d is a monotonically increasing function of both M and N, which means larger M and N values lead to higher detection accuracy.

As for the complexity analysis, the number of complex multiplications is only considered since they are computationally most intensive. To have a deep insight, we include recently proposed methods in [4], [6], and [8] for comparison. The results are listed in Table I.

B. Relation With the Eigenvalue-Based Algorithm in [2]

Among existing methods, the most relevant to our proposed scheme is the one presented in [2]. Motivated by this, we will next compare this detection method with the proposed one.

There are two eigenvalue-based detectors proposed in [2], of which the decision metrics are

$$\frac{\max_i \lambda_i}{\min_j \lambda_j} \quad \text{and} \quad \frac{\frac{1}{N}\sum_{i=0}^{N-1}\lambda_i}{\min_j \lambda_j} \tag{17}$$

respectively, where λ_i $\{i = 1, \ldots N\}$ is the ith eigenvalue of the covariance matrix. While our method measures the off-diagonal power of the covariance matrix, the decision metrics in (17) are based on the ratio of the maximum eigenvalue to the minimum and that of the average eigenvalue to the minimum, respectively. Although (17) can be extended to OFDM systems, it is shown in [14] that null subcarriers and fading channels can cause the covariance matrix to be rank-deficient, which means some eigenvalues would be zero or close to zero. Obviously, in this situation, the detection results will be unreliable since decision metrics in (17) apply the minimum eigenvalue as denominators, which can result in numerical instability.

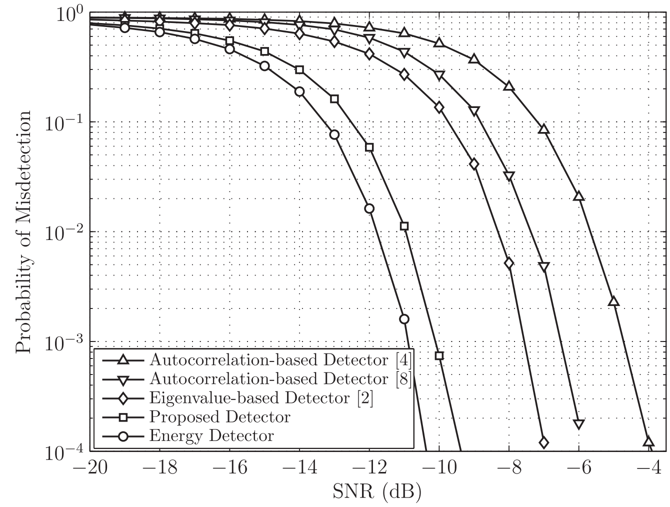

Fig. 1. P_{md} of the comparative algorithms over the AWGN channel.

V. NUMERICAL RESULTS

We consider a scenario similar to the IEEE 802.11a standard, i.e., $N = 64$ and $N_g = 16$. The normalized CFO is evenly distributed over (− 0.5, 0.5], and the perfect timing is assumed. We consider the additive white Gaussian noise (AWGN) and frequency-selective channels, including the SUI-3 and SUI-4 models [15]. Source symbols are modulated using quadrature phase-shift keying. The observation window contains 50 symbols. The energy detector (ED), the eigenvalue-based detector (EBD) [2], and two autocorrelation-based detectors (ABDs) [4], [8] are simulated for performance comparison with respect to the proposed scheme. The ED assumes perfect knowledge of the noise variance, and therefore, its performance is optimal and offers a baseline for comparison.

Fig. 1 shows the probability of misdetection P_{md}, which is defined as $P_{\text{md}} = 1 - P_d$, over the AWGN channel where P_{fa} is set to 10%. The null subcarriers with indices $\{3-4\}$ and $\{61-62\}$ are used to estimate the noise variance for the proposed method. It is not surprising that the ED performs the best but would see a severe performance loss in the presence of a noise uncertainty. Except for the ED, the proposed method provides a better performance than the other algorithms, whereas the ABD in [4] is subjected to the highest error probability since the correlation incurred by the CP that this algorithm relies on could be destroyed by the CFO. For instance, the performance gain of our scheme over the EBD and the two ABDs is about 2.5, 3.8, and 5.5 dB, respectively, at $P_{\text{md}} = 10^{-3}$. Although it is possible that the other methods could include more symbols in the observation window to achieve a lower P_{md}, it is disadvantageous in situations where the sensing time requirement is stringent.

Figs. 2 and 3 show the P_{md} of different algorithms over SUI-3 and SUI-4 channels, respectively, and the P_{fa} is also set to 10%. The fact that all the five methods witness a lower P_{md} over SUI-3 than SUI-4 demonstrates that the frequency selectivity of the multipath channel has a negative effect on spectrum sensing. As before, both Figs. 2 and 3 confirm that the proposed algorithm is superior over the EBD and

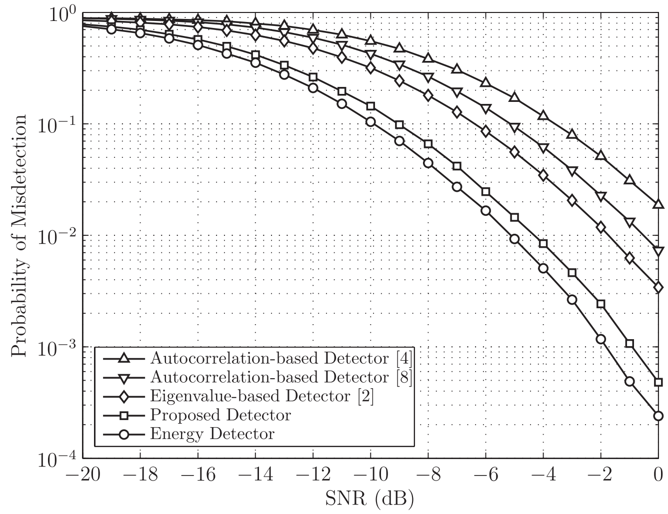

Fig. 2. P_{md} of the comparative algorithms over the SUI-3 channel.

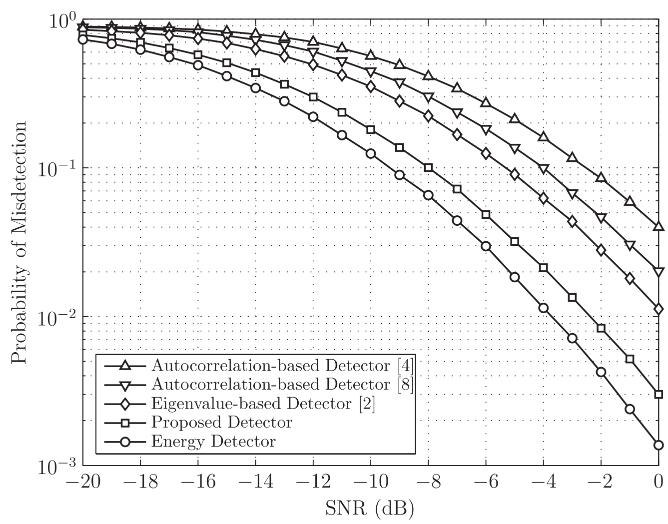

Fig. 3. P_{md} of the comparative algorithms over the SUI-4 channel.

ABDs in the sense that it always has the lowest P_{md} over the whole SNR range, except for the ED. The performance of the EBD may suffer from the rank-deficient covariance matrix caused by channel nulls. In addition, ABDs in [4] and [8] are subjected to further performance loss because the correlation incurred by the CP is further destroyed by the multipath fading. However, the EBD is more robust to the frequency offset than two ABDs.

Fig. 4 plots the receiver operating characteristic (ROC) curves of different methods over SUI-4 channel, where $\mathrm{SNR} = -10$ dB. As can be observed from the figure, except for the ED, the proposed algorithm has the optimal curve, where P_d increases notably with little increase of P_{fa}, particularly when P_{fa} is small. On the other hand, the EBD is superior over two ABDs as the EBD's decision metric is more robust to the channel fading and CFO than that of two ABDs.

VI. Conclusion

This paper has proposed a new spectrum sensing algorithm for OFDM signals contaminated by the CFO in CR systems. This scheme is of high bandwidth utilization as it requires no training symbols or pilot tones. A new decision metric was introduced to measure the off-diagonal power of the signal covariance matrix. Given the predefined P_{fa}, we derived the threshold that depends on the number of subcarriers N, the length of symbols M, and the noise variance. It was shown both theoretically and numerically that the proposed sensing is robust to the CFO, which makes it practical for real applications. Moreover, although the proposed algorithm is designed for use in scenarios with frequency offsets, it still works in the absence of this error. Numerical simulation results demonstrated that the proposed scheme outperforms several existing methods in terms of the probability of misdetection.

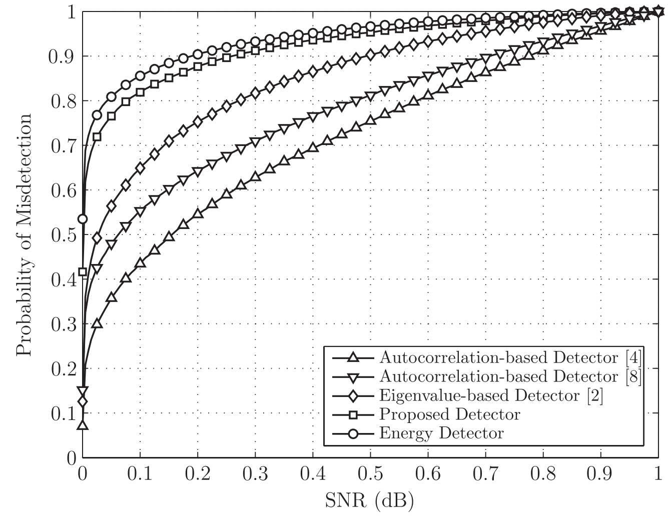

Fig. 4. ROC curves of the comparative algorithms over the SUI-4 channel.

Appendix A
Derivation of the PDFs in (10) and (13)

The detector's input is $r_{i,n} = w_{i,n}$ under $\mathcal{H}_0$; thus, the (p,q)th off-diagonal element of the covariance matrix is $\hat{\mathbf{R}}(p,q) = (1/M)\sum_{i=0}^{M-1} W_{i,p}W_{i,q}^*$. According to the CLT, $\hat{\mathbf{R}}(p,q)$ is Gaussian distributed if M is large enough. Therefore, the decision metric ζ in this situation is essentially the sum of K i.i.d. Rayleigh random variables, of which the pdf is approximated as

$$p(\zeta|\mathcal{H}_0) \approx \frac{1}{\sqrt{2\pi}} e^{-\frac{1}{2}\left(\frac{\zeta - \mu_{\mathcal{H}_0}\sqrt{K}}{\sigma_{\mathcal{H}_0}}\right)^2} + f_e(\zeta) \tag{A.1}$$

where $\mu_{\mathcal{H}_0}$ and $\sigma^2_{\mathcal{H}_0}$ are the mean and variance of $|\hat{\mathbf{R}}(p,q)|$, respectively. $f_e(\zeta)$ compensates for the error of approximation when K is small. Since $K = (N^2 - N)/2$ is usually a large number, $f_e(\zeta)$ can be ignored. Given $\mu_{\mathcal{H}_0} = \sqrt{\pi/4M}\sigma_n^2$ and $\sigma^2_{\mathcal{H}_0} = (1-(\pi/4))\sigma_n^4/M$, we can obtain (10).

As for (13), the corresponding (p,q)th entry of the sample covariance matrix is given by

$$\hat{\mathbf{R}}(p,q) \approx \frac{1}{M}\sum_{i=0}^{M-1}\left[W_{i,p}H^*_{i,q-\varepsilon}X^*_{i,q-\varepsilon} \right. \\ \left. + W_{i,q}H^*_{i,p-\varepsilon}X^*_{i,p-\varepsilon} + W_{i,p}W^*_{i,q}\right]. \tag{A.2}$$

$\hat{\mathbf{R}}(p,q)$ can be approximated as a complex Gaussian variable if M is large enough, with its mean and variance being $\mu = 0$ and $\sigma^2 \approx (\sigma_n^4 + 2\sigma_n^2\sigma_H^2)/M$, where σ_H^2 is the variance of the channel frequency response. Therefore, ζ under $\mathcal{H}_1$ in this scenario is a sum of multiple i.i.d. Rayleigh variables. With the results in [10] and [16, pp. 295], (13) can be obtained.

APPENDIX B
DERIVATION OF THE PDF IN (14)

In the presence of CFO, the kth output of the ith OFDM symbol after DFT is (6). The variance of $\hat{\mathbf{R}}(p,q)$ is approximated by σ_n^4/M as the detector often operates at SNR $\ll 0$ dB. As for the calculation of the mean, the components contributed are presented by

$$\mathrm{E}\left\{\hat{\mathbf{R}}(p,q)\right\} = \mathrm{E}\left\{\sum_{t=0}^{N-1} I_{t-p}^{\varepsilon} I_{l-q}^{\varepsilon\,*} |H_{i,t}|^2\right\}. \tag{B.1}$$

The other components in $\hat{\mathbf{R}}(p,q)$ are ignored due to a zero mean. It can be verified that

$$\sum_{p=0}^{N-1} \sum_{q=0,\, p\neq q}^{N-1} \sum_{t=0}^{N-1} I_{t-p}^{\varepsilon} I_{t-q}^{\varepsilon\,*} = N\left(\left|\sum_{n=0}^{N-1} I_n^{\varepsilon}\right|^2 - \sum_{n=0}^{N-1} |I_n^{\varepsilon}|^2\right). \tag{B.2}$$

The mean of (B.2) can be obtained with numerical methods by integrating over $\varepsilon \in (-0.5, 0.5]$, which is $(4\pi^2\sigma_H^2 N)/((\Gamma+\psi(N))^2 + \psi(1,N) - \pi^2/6)$. Then, the amplitude $|\hat{\mathbf{R}}(p,q)|$ in this case is Ricean distributed because of the nonzero mean. Again, since the decision metric is the sum of Ricean variables, the pdf in the presence of the primary user's signal can be approximated as [10]

$$p(\zeta|\mathcal{H}_1) \approx \frac{1}{\sqrt{2\pi}} e^{-\frac{1}{2}\left(\frac{\zeta-\mu_{\mathcal{H}_1}\sqrt{K}}{\sigma_{\mathcal{H}_1}}\right)^2} \tag{B.3}$$

where $\mu_{\mathcal{H}_1} = \sigma\sqrt{\pi/2}\ \ L_{1/2}(-\mu^2/2\sigma^2)$, and $\sigma_{\mathcal{H}_1}^2 = 2\sigma^2 + \mu^2 - (\pi\sigma^2/2)L_{1/2}^2(-\mu^2/2\sigma^2)$. Up to this point, (14) can be obtained.

REFERENCES

[1] T. Yucek and H. Arslan, "A survey of spectrum sensing algorithms for cognitive radio applications," *IEEE Commun. Surveys Tuts.*, vol. 11, no. 1, pp. 116–130, 1st Quart. 2009.

[2] Y. Zeng and Y.-C. Liang, "Eigenvalue-based spectrum sensing algorithms for cognitive radio," *IEEE Trans. Commun.*, vol. 57, no. 6, pp. 1784–1793, Jun. 2009.

[3] E. Axell, G. Leus, and E. G. Larsson. "Overview of spectrum sensing for cognitive radio," in *Proc. Int. Workshop Cognitive Inf. Process.*, Elba Island, Italy, Jun. 2010, pp. 322–327.

[4] Z. Lei, F. Chin, and P. S. Chin, "Sensing OFDM systems under frequency-selective fading channels," *IEEE Trans. Veh. Technol.*, vol. 59, no. 4, pp. 1960–1968, May 2010.

[5] S. Bokharaiee, H. H. Nguyen, and E. Shwedyk, "Blind spectrum sensing for OFDM-based cognitive radio systems," *IEEE Trans. Veh. Technol.*, vol. 60, no. 3, pp. 858–871, Mar. 2011.

[6] H.-S. Chen, W. Gao, and D. G. Daut, "Spectrum sensing for OFDM systems employing pilot tones," *IEEE Trans. Wireless Commun.*, vol. 8, no. 12, pp. 5862–5860, Dec. 2009.

[7] H.-S. Chen and W. Gao, "Spectrum sensing for TV white space in North America," *IEEE J. Sel. Areas Commun.*, vol. 29, no. 2, pp. 316–326, Feb. 2011.

[8] Z. Chen, T. Luan, and X. D. Zhang, "Sensing orthogonal frequency division multiplexing systems for cognitive radio with cyclic prefix and pilot tones," *IET Commun.*, vol. 6, no. 1, pp. 97–106, Jan. 2012.

[9] Y. H. Zeng, Y.-C. Liang, and T.-H. Pham, "Spectrum sensing for OFDM signals using pilot induced auto-correlations," in *IEEE J. Sel. Areas Commun.*, vol. 31, no. 3, pp. 353–363, Mar. 2013.

[10] J. A. Lopez-Salcedo, "Simple closed-form approximation to Ricean sum distributions," *IEEE Signal Process. Lett.*, vol. 16, no. 3, pp. 153–155, Jun. 2009.

[11] S. M. Kay, *Fundamentals of Statistical Signal Processing, Detection Theory*. Upper Saddle River, NJ, USA: Prentice-Hall, 1993.

[12] Y. H. Zeng, S. W. Oh, and R. H. Mo, "Subcarrier sensing for distributed OFDMA in powerline communication," in *Proc. IEEE Int. Conf. Commun.*, Dresden, Germany, Jun. 2009, pp. 1–5.

[13] M. Speth, S. A. Fechtel, G. Fock, and H. Meyr, "Optimum receiver design for wireless broad-band systems using OFDM—Part I," *IEEE Trans. Commun.*, vol. 47, no. 11, pp. 1668–1677, Nov. 1999.

[14] X. Ma, C. Tepedelenlioglu, G. B. Giannakis, and S. Barbarossa, "Non-data-aided carrier offset estimators for OFDM with null subcarriers: Identifiability, algorithms, and performance," *IEEE J. Sel. Areas Commun.*, vol. 19, no. 12, pp. 2504–2515, Dec. 2001.

[15] V. Erceg *et al.*, "Channel models for fixed wireless applications," IEEE 802.16 broadband wireless working group, IEEE802.16a-03/01, Tech. Rep., 2003.

[16] K. Krishnamoorthy, *Handbook of Statistical Distributions With Applications*. Boca Raton, FL, USA: CRC Press, 2006.

Completely Irrepressible Sequences for Multiple-Packet Reception

Yijin Zhang, *Member, IEEE*, Yuan-Hsun Lo, and Wing Shing Wong, *Fellow, IEEE*

***Abstract*—In this paper, we study completely irrepressible (CI) sequences. For a slot-asynchronous communication system supporting K users with such sequences, a key feature is that each user is guaranteed to be able to send out at least one contention-free packet in one common sequence period. This is a desirable property since it provides a bounded delay guarantee for medium access control (MAC) layer contention, in contrast to random access schemes. Generalizing previous studies on CI sequences, we investigate systems endowed with multiple-packet reception (MPR) capability γ, $2 \leq \gamma < K$. That is, a packet transmission is successful if and only if the total number of transmissions in the channel at any point in time during its transmission is less than or equal to γ. We investigate the minimum period L of CI sequences for MPR as L is a fundamental factor that affects the worst-case delay. The main result is that L is asymptotically upper bounded by $2K^2/(\gamma-2)$ when $\gamma \geq 3$. For $\gamma = 2$, the corresponding bound is $2K^2$. In contrast, the bound for the single-packet reception system ($\gamma = 1$) is $4K^2$. Simulation results verify our analysis and present comparative studies between CI sequences and random access in an application of group-based detection in a wireless sensor network.**

***Index Terms*—Collision channel, multiple-packet reception (MPR), protocol sequences, time synchronization.**

I. INTRODUCTION

A. Background and Motivation

Protocol sequences were originally proposed by Massey and Mathys [1] to demonstrate that the reliable medium access control (MAC) protocol can be defined without a feedback link. Protocol-sequence-based access schemes recently have drawn much attention

Manuscript received December 5, 2014; revised June 22, 2015; accepted August 31, 2015. Date of publication September 15, 2015; date of current version August 11, 2016. This work was supported in part by the Hong Kong Research Grant Council under Earmarked Grant CUHK414012, by the National Natural Science Foundation of China under Grant 61301107 and Grant 61174060, and by the Shenzhen Knowledge Innovation Program under Grant JCYJ20130401-172046453. The review of this paper was coordinated by Dr. H. Jiang.

Y. Zhang is with the School of Electronic and Optical Engineering, Nanjing University of Science and Technology, Nanjing 210094, China (e-mail: yijin.zhang@gmail.com).

Y.-H. Lo is with the Department of Mathematics, National Taiwan Normal University, Taipei 106, Taiwan (e-mail: yhlo0830@gmail.com).

W. S. Wong is with the Department of Information Engineering, Chinese University of Hong Kong, Shatin, Hong Kong, and also with Chinese University of Hong Kong Shenzhen Research Institute, Shenzhen 518000, China (e-mail: wswong@ie.cuhk.edu.hk).

Color versions of one or more of the figures in this paper are available online at http://ieeexplore.ieee.org.

Digital Object Identifier 10.1109/TVT.2015.2478895